

Paper

# Analysis of the optical second harmonic generation from Pt nanowires on the faceted MgO(110) template

Yoichi Ogata, Nguyen Anh Tuan, Saho Takase and Goro Mizutani\*

Japan advanced Institute of Science and Technology

1-1 Asahidai, Nomi, Ishikawa 923-1292, Japan

\*mizutani@jaist.ac.jp

(Received : October 3, 2010; Accepted : November 29, 2010)

We have measured optical second harmonic (SH) intensity from Pt nanowires with modified ellipsoidal cross sections on the MgO(110) faceted template. The observed SH intensity patterns as a function of the sample rotation angle  $\varphi$  around the surface normal were characterized by the effective nonlinear susceptibility arising from  $C_s$  symmetry of the Pt nanowires. The effective nonlinear susceptibility element  $\chi_{222}$  was observed dominantly with the suffix 2 representing the [110] direction of the MgO substrate. Other nonlinear susceptibility elements were also detected and their origins are discussed.

## 1. Introduction

One-dimensional nanostructured metals have attracted great attention because of their potential applications to ultrafast optical switching and wavelength conversion devices [1,2]. In many of these applications, nonlinear optical effects are playing an important role. Especially, much effort has been paid to investigate their optical second harmonic (SH) response [3,4]. By understanding the basic principles of such phenomenon in low-dimensional materials, the development of the related application field must be promoted.

Recently, we have observed the cross sections of Pt nanowires deposited on the MgO(110) faceted template by transmission electron microscopy (TEM) and investigated their SH response [5]. We found that the nonlinear susceptibility element  $\chi_{222}$  arising from the symmetry breaking of the cross sectional shapes of the nanowires in direction 2:  $[\bar{1}\bar{1}0]$  is dominant in the SHG for the *s*-in/*s*-out polarization combination. However, the relation between the local asymmetry of the platinum cross-sectional shapes and the SH efficiency could not be completely analyzed because there was a large scatter in the SH intensity and it made the theoretical fitting unreliable.

In this work, we have reduced the scatter in the SHG response of the same nanowires by

increasing the measurement time. Theoretical decomposition of the SH intensity patterns into contributions of different nonlinear susceptibility elements was also obtained. By using this method, the relationship between the shapes of the nanowire and nonlinear optical property became clearer than in our previous work. Especially, we analyzed the SH pattern for *p*-in/*p*-out polarization configuration in order to discuss the effect of the cross-sectional shapes other than the effect of the broken symmetry in direction 2.

## 2. Experimental

Pt nanowires with modified ellipsoidal cross sections on MgO(110) substrate were prepared by shadow deposition at 750°C in UHV chamber of  $9.5 \times 10^{-7}$  Pa [5]. The shapes of the Pt nanowires were observed by TEM as shown in Fig.1. According to the expanded TEM image of nanowires in Fig. 1(a), the Pt nanowires with 7 nm width seen in dark contrast run in direction 1 on the MgO(110) faceted template. Hereafter, the numbers 1, 2, and 3 represent the [001],  $[\bar{1}\bar{1}0]$ , and [110] directions on the MgO(110) template, respectively, as shown in Fig. 1(b). Figure 1(b) is expanded cross-sectional TEM images of Pt nanowires. As shown in the more expanded image of a single nanowire in the inset of Fig. 1(b), the shape of the metal on the top of the MgO facet marked as (A) has larger curvature and

sharpness than the other parts such as that marked as (B).

The measurement setup of SHG was already reported elsewhere [5]. We used a frequency-doubled mode-locked  $\text{Nd}^{3+}$ : YAG laser at the photon energy of  $2.33 \text{ eV}$  in order to excite SHG in the nanowires. The pulse energy was set at  $120 \mu\text{J}$ . The SH intensity as a function of the azimuthal angle around the surface normal was measured in the reflection direction with the incident angle of  $45^\circ$ . The reflected SH light was passed through a monochromator and detected by a photomultiplier. In order to compensate for the sensitivity variation of the optical system as a function of the wavelength,  $\alpha\text{-SiO}_2(0001)$  plate was used as a reference sample. The measurement was done for the azimuthal angle of every  $10 \text{ deg}$  and for four different polarization combinations. In order to get high signal-to-noise ratio of the SH intensity, the SH light pulse was accumulated for 12 hours for each SH intensity pattern in Fig. 2.

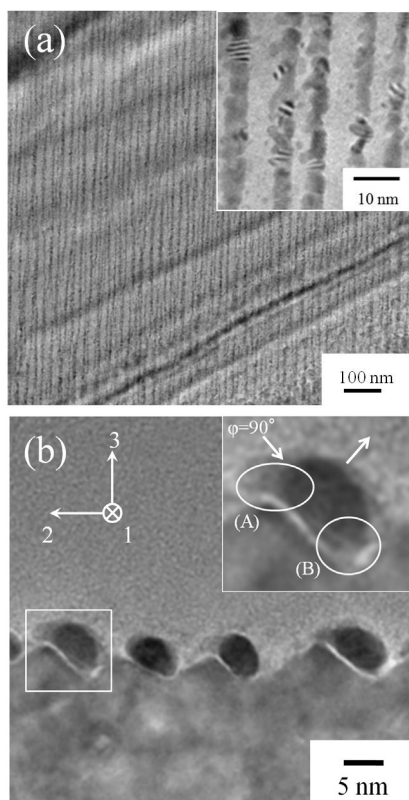


Fig.1. (a) Plan-view and expanded TEM images of the Pt nanowires on the MgO(110) faceted template. Nanowires seen in dark contrast run in the  $1; [001]$  direction. (b) The cross sectional TEM and expanded images of the Pt nanowires. The arrows in the upper right inset shows excitation and emitted light wave vector for  $\phi=90^\circ$ . In (A) a part of the platinum is seen to reach the top of the facet. In (B) the shape of the platinum is determined by the MgO faceted template.

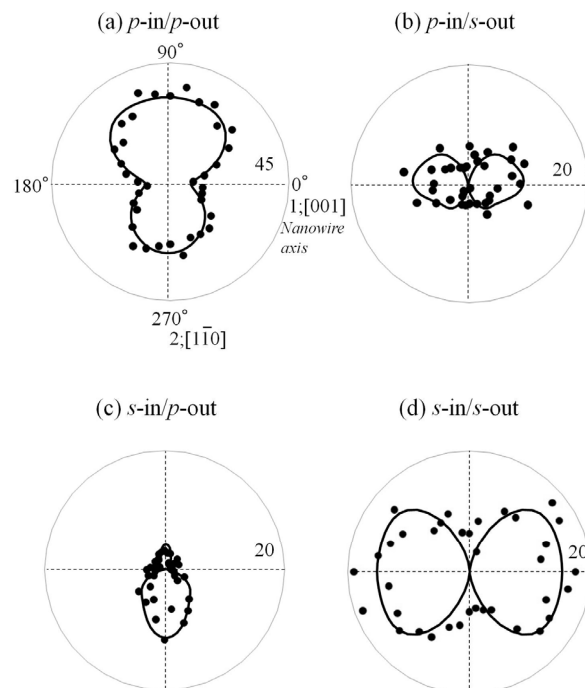


Fig.2 Angular SH intensity patterns for Pt nanowires on the MgO(110) faceted template as a function of the sample rotation angle  $\phi$  for four polarization combinations. The measured (filled circles) SH intensity patterns are fitted to the calculated (solid line) theoretical intensity SH curves.

### 3. Results and discussion

Figure 2 shows the polar plots of SH intensity from the Pt nanowire array (filled circle) on the MgO(110) substrate as a function of the sample rotation angle  $\phi$  around the surface normal and for four different polarization combinations. In our previous work, theoretical curves were tentatively fitted to the experimental SH data, but the fitting was rather unreliable due to the fluctuation of the SH intensity as a function of the angle  $\phi$ . In the present work, the number of pulse irradiation was increased by 4 times in order to obtain improved signal-to-noise ratio.

The SH intensity from the nanowires in Fig. 2 depends strongly on the rotation angle  $\phi$ . The patterns show two lobes at  $\phi=90^\circ$  and  $270^\circ$  with different intensities in the  $p\text{-in}/p\text{-out}$  configuration in Fig.2(a), two smaller lobes at  $\phi=0^\circ$  and  $180^\circ$  in the  $p\text{-in}/s\text{-out}$  configuration in Fig.2(b), one lobe at  $\phi=270^\circ$  in the  $s\text{-in}/p\text{-out}$  configuration in Fig.2(c), and two lobes of the same intensities at  $\phi=0^\circ$  and  $180^\circ$  in the  $s\text{-in}/s\text{-out}$  configuration in Fig.2(d). All the SH intensity patterns have a mirror symmetry with respect to the line including the  $\phi=90^\circ$  and  $270^\circ$  directions.

$ijk$	$p$ -in/ $p$ -out	$p$ -in/ $s$ -out	$s$ -in/ $p$ -out	$s$ -in/ $s$ -out
113				
223				
121				
211	.			.
222				
233	.	-		
311	-		.	

Fig.3 Calculated SH intensity patterns decomposed into the contributions of different nonlinear susceptibility elements.

We have analyzed the SH intensity patterns from the Pt nanowires by using a phenomenological model [6]. We have first fitted the theoretical curve to the experimental value by a least square fitting program assuming  $C_s$  symmetry for the Pt nanowires/MgO(110) system. Here, ten independent nonlinear susceptibility elements are permitted for the Pt nanowires of  $C_s$  symmetry [7]. We have already obtained theoretical SH intensity patterns when one of the ten independent nonlinear susceptibility elements are set equal to a certain finite value and all the other elements are set equal to zero. The theoretical SH pattern is a linear combination of the patterns in the complex plane with the multiplication factors of nonlinear susceptibility  $\chi_{ijk}$ .

Following the similar phenomenological fitting of Pt nanowires on NaCl(110) faceted template [8], we assume  $\chi_{333}$  and  $\chi_{323}$  to be zero in order to avoid meaningless negative interference between the susceptibility elements. In addition, we assume that  $\chi_{322}$  is almost zero. This is because the SH intensity pattern for  $s$ -in/ $p$ -out polarization configuration in Fig. 2(c) have vanishing intensity at  $\varphi=0^\circ$  and  $180^\circ$ , while the element  $\chi_{322}$  should show the biggest intensity at  $\varphi=0^\circ$  and  $180^\circ$ . Eventually we analyzed the contributions of seven independent nonlinear susceptibility elements. The calculated patterns by a fitting program reproduce the experiment

well as seen as the solid curves in Fig. 2. Therefore it is reasonable to discuss the physical meaning of the observed nonlinear susceptibility elements. Figure 3 shows the decomposition of the calculated SH intensity patterns into the contributions of different nonlinear susceptibility elements  $\chi_{ijk}$ .

As we can see in the inset of Fig. 1(b) the cross-sectional shapes of the Pt nanowires has a broken symmetry in directions 2 and 3. Then the nonlinear susceptibility element including odd numbers of suffices 2 and 3 arises due to the symmetry breaking in these directions. In the present case there are four nonlinear susceptibility elements  $\chi_{121}$ ,  $\chi_{211}$ ,  $\chi_{222}$ , and  $\chi_{233}$  due to the broken symmetry in direction 2. We also have three nonlinear susceptibility elements  $\chi_{311}$ ,  $\chi_{113}$ , and  $\chi_{223}$  arising from the broken symmetry in direction 3.

The SH intensity pattern for  $p$ -in/ $p$ -out polarization combination is dominated by the interference between signals arising from the  $\chi_{113}$ ,  $\chi_{223}$  and  $\chi_{222}$  elements as we can see in Fig. 3. The elements of  $\chi_{113}$  and  $\chi_{223}$  originate from the broken symmetry in direction 3, and  $\chi_{222}$  originates from the broken symmetry in direction 2. Thus we can say that the pattern for this polarization combination should be sensitive to the shape of the cross section of the nanowires.

The calculated patterns in Fig. 3 of the nonlinear susceptibility element  $\chi_{211}$  are similar to those of the experimental patterns observed in  $p$ -in/ $s$ -out and  $s$ -in/ $p$ -out polarization configurations in Fig. 2(b) and (c), respectively. We can say that the broken symmetry in direction 2 can be picked up in these polarization configurations in the present case.

Finally, let us see the SH intensity pattern in  $s$ -in/ $s$ -out polarization configuration. The SH intensity pattern has two clear lobes at  $\varphi=0^\circ$  and  $180^\circ$ . In Fig. 3 we see that the contribution of  $\chi_{222}$  is more predominant than the other two elements  $\chi_{121}$  and  $\chi_{211}$ . We can say that the SH intensity at  $\varphi=0^\circ$  and  $180^\circ$  solely reflects the contribution of  $\chi_{222}$  and hence of the broken symmetry in the direction 2. As we pointed out in our previous work, the broken symmetry is considered to occur at the asymmetric part marked as (A) in Fig.1(b).

#### 4. Conclusion

We have measured azimuthal angle dependence of the optical second harmonic intensity from Pt nanowires on a MgO(110) faceted template, with good signal-to-noise ratio. From the obtained SH intensity patterns the

contribution of the effective nonlinear susceptibility elements of the Pt nanowires was determined.

#### Acknowledgements

We thank A. Sugawara of Hitachi Co. Limited for his support in the sample preparation, and K. Higashimine of JAIST Nanotechnology Center for his support in our TEM observation. This work was conducted in Kyoto-Advanced Nanotechnology Network, supported by "Nanotechnology Network" of the Ministry of Education, Culture, Sports, Science and Technology (MEXT), Japan.

#### References

[1] T. M. Whitney, P. C. Searson, J. S. Jiang, and C. L. Chein, *Science* **261**, 1316, (1993).

[2] H. Pan, W. Chen, Y. P. Feng, and W. Ji, *Appl. Phys. Lett.* **88**, 223106, (2006).

[3] T. Kitahara, A. Sugawara, H. Sano, and G. Mizutani, *Appl. Surf. Sci.* **219**, 271, (2003).

[4] K. Locharoenrat, A. Sugawara, S. Takase, H. Sano, and G. Mizutani, *Surf. Sci.* **601**, 4449, (2007).

[5] Y. Ogata, N. A. Tuan, S. Takase, and G. Mizutani, *Surf. Interface. Anal.* **42**, 1663, (2010).

[6] E. Kobayashi, G. Mizutani, S. Ushioda, *Jpn. J. Appl. Phys.* **36**, 7250, (1997).

[7] P.-F. Brevet, Surface Second Harmonic Generation, Press Polytechniques et Universitaires Romandes, Lausanne, p. 48, (1997).

[8] N. Hayashi, K. Aratake, R. Okushio, T. Iwai, A. Sugawara, H. Sano, and G. Mizutani, *Appl. Surf. Sci.* **253**, 8933, (2007).